

ON THE DEVELOPMENT OF SYNOPTIC-SCALE DISTURBANCES OVER THE SUBTROPICAL OCEANS

STANLEY L. ROSENTHAL

National Hurricane Research Laboratory, ESSA, Miami, Fla.

ABSTRACT

Disturbances with scales of a few thousand kilometers are commonly observed in the troposphere over the subtropical oceans. Synoptic experience seems to indicate that many of these large-scale disturbances are driven by latent heat released in organized convection. To explore this possibility, a series of numerical experiments were conducted with a simple, two-layer, quasi-geostrophic model. The convective heating function was treated in the same manner as that employed by various investigators in recent studies of hurricane dynamics. In this formulation, convection is controlled by frictional convergence in the Ekman layer. These numerical experiments show that this heating mechanism, within the framework of the simple dynamical model employed, can produce significant intensification of large-scale disturbances.

1. INTRODUCTION

Synoptic experience in subtropical latitudes indicates that the release of latent heat in organized convection may be responsible not only for the development of relatively small-scale systems such as hurricanes but also for larger-scale disturbances such as those discussed by Riehl [7] and Frank [3]. A characteristic feature of these synoptic situations seems to be the simultaneous growth of a low tropospheric trough or cyclone and an upper tropospheric anticyclone centered somewhat to the east of the low-level cyclonic system.

The present paper is an attempt to provide a theoretical framework within which the growth of such disturbances can be discussed. The convective heating function is modeled according to the ideas set forth by Charney and Eliassen [2], Ooyama [6], Kuo [4], Ogura [5], and others who take the presence or absence of deep cumulus convection over the subtropical oceans to be dependent upon the presence or absence of convergence in the Ekman layer. The stability of circularly symmetric vortices on an f -plane subject to convection governed by Ekman layer convergence has been treated by the authors cited above. The disturbances to be considered here, however, are too large in scale to allow the β -effect to be neglected.

Considered within the framework of the classical eigenvalue stability analysis, the study of growth due to convective heating, subject to β -plane dynamics, is, for a number of reasons, extremely difficult. To avoid these difficulties, a less sophisticated and far less satisfying technique, the numerical, initial-value approach, is employed here. The dynamics are simplified through the

utilization of a quasi-geostrophic model. This is justifiable since we are concerned with subtropical (not equatorial) motions. At 20° lat., for example, the Rossby number appropriate to a characteristic scale of 1000 km. and a characteristic wind of 10 m. sec.^{-1} is 0.2.

2. THE MODEL

For simplicity, we adopt a two-level, quasi-geostrophic model (see fig. 1), neglect meridional variations of the velocity components, and linearize on a stagnant base state. The pertinent equations are the vorticity equations at levels 1 and 3,

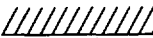




<u>PRESSURE</u>	<u>LEVEL</u>		<u>VARIABLES</u>	<u>EQUATIONS</u>
000MB.	0		$\omega_0 = 0$	
250MB.	1		ϕ_1	VORTICITY
500MB.	2		ω_2	HYDROSTATIC THERMODYNAMIC CONTINUITY
750MB.	3		ϕ_3	VORTICITY
1000MB.	4		$\omega_4 = 0$	

FIGURE 1.—Vertical structure of the two-level, quasi-geostrophic model.

$$\frac{\partial^3 \phi_1}{\partial x^2 \partial t} + \beta \frac{\partial \phi_1}{\partial x} = \frac{2f_0^2 \omega_2}{p_4} \quad (1)$$

$$\frac{\partial^3 \phi_3}{\partial x^2 \partial t} + \beta \frac{\partial \phi_3}{\partial x} = \frac{2f_0^2}{p_4} (\omega_4 - \omega_2) \quad (2)$$

and the thermodynamic equation at level 2,

$$\frac{\partial(\phi_3 - \phi_1)}{\partial t} + \frac{\sigma_2 p_4}{2} \omega_2 = -\frac{R}{c_p} \dot{Q}_2 \quad (3)$$

where

$$\sigma_2 = -\left(\frac{\alpha}{\theta} \frac{\partial \theta}{\partial p}\right)_2 \quad (4)$$

is the base-state static stability at 500 mb. \dot{Q}_2 is the heat added per unit mass and time at level 2. The remaining notation is standard. After Charney and Eliassen [1], the frictional vertical motion at level 4 is evaluated from Ekman theory and for our purposes may be written

$$\omega_4 = -\lambda \frac{\partial^2 \phi_3}{\partial x^2} \quad (5)$$

$$\lambda = \frac{\rho_4 g D_E l^* \sin 2\psi}{2f_0} \quad (6)$$

ρ_4 is the 1000-mb. density, $D_E = (2A^*/f_0)^{1/2}$ is a measure of the depth of the Ekman layer, A^* is the kinematic coefficient of eddy viscosity, ψ is the angle between the wind and geopotential contours at 1000 mb., and l^* is the ratio between wind speeds at 1000 mb. and 750 mb.

From the previous section,

$$\dot{Q}_2 = 0 \text{ when } \omega_4 \geq 0. \quad (7a)$$

After Ogura [5], the heating function is defined by

$$\left(\frac{\theta}{c_p T}\right)_2 \dot{Q}_2 = \eta \left(\frac{\partial \theta}{\partial p}\right)_2 \omega_4 \text{ when } \omega_4 < 0. \quad (7b)$$

(η is identical to Ooyama's [6] entrainment parameter (value probably between 2 and 4).) To avoid unlimited growth of the perturbations (see Kuo [4]), we add the condition

$$\dot{Q}_2 = 0 \text{ when } (T_s - T)_2 \leq 0 \quad (7c)$$

where T_s is the temperature along the pseudo-adiabat through the lifting condensation level of the surface air. Physically, condition (7c) implies that the convective scale provides a heat source for the large-scale flow only as long as the cumuli are warmer than their environment.

In view of the simple vertical structure of the model (fig. 1), the temperatures used in (7c) should be considered averages over the 250–750-mb. layer. The various assumptions and physical concepts involved in the derivation of (7a, 7b, 7c) are discussed in detail in [2, 4, 5, 6] and will not be repeated here.

By use of (4), equation (7b) may be written

$$\dot{Q}_2 = -\frac{c_p p_4 \sigma_2 \eta \omega_4}{2R} \text{ when } \omega_4 < 0. \quad (7b)$$

If we eliminate ω_2 between (1), (2), and (3) and make use of (5) and (7b), we obtain

$$\frac{\partial^3 \phi_3}{\partial x^2 \partial t} = -\nu \frac{\partial^2 \phi_3}{\partial x^2} - \beta \frac{\partial \phi_3}{\partial x}, \quad (8)$$

$$\frac{\partial^3 \phi_D}{\partial x^2 \partial t} - \gamma^2 \frac{\partial \phi_D}{\partial t} = \nu(2\eta - 1) \frac{\partial^2 \phi_3}{\partial x^2} - \beta \frac{\partial \phi_D}{\partial x}, \quad (9)$$

where

$$\phi_s = \phi_1 + \phi_3, \quad (10)$$

$$\phi_D = \phi_3 - \phi_1, \quad (11)$$

$$\gamma^2 = 8f_0^2 / \sigma_2 p_4^2, \quad (12)$$

$$\nu = 2f_0^2 \lambda / p_4 \quad (13)$$

and it is understood that $\eta = 0$ when $\dot{Q}_2 = 0$.

3. INITIAL CONDITIONS

At the initial instant, we take

$$\phi_3 = -A \cos kx, \quad A > 0, \quad (14)$$

$$\phi_1 = -MA \cos(kx + \delta), \quad M > 0, \delta > 0. \quad (15)$$

M is the ratio of initial amplitudes at levels 1 and 3 and δ is the initial phase lag between these levels. From (5), (14), and (7b), the convective region at the initial instant is

$$\frac{\pi}{2k} > x > -\frac{\pi}{2k} \quad (16)$$

provided that $(T_s - T)_2 > 0$. Lacking synoptic information concerning reasonable choices for M and δ , we proceed as follows.

The kinetic energy, averaged over a wavelength, at level 1 is

$$K_1 = \frac{1}{2f_0^2 L} \int_{-L/2}^{L/2} \left(\frac{\partial \phi_1}{\partial x}\right)^2 dx, \quad (17)$$

at level 3,

$$K_3 = \frac{1}{2f_0^2 L} \int_{-L/2}^{L/2} \left(\frac{\partial \phi_3}{\partial x}\right)^2 dx. \quad (18)$$

The kinetic energy averaged both vertically and over a wavelength is

$$K = K_1 + K_3. \quad (19)$$

Note that

$$L = \frac{2\pi}{k} \tag{20}$$

The time rates of change of these quantities are given by

$$\frac{\partial K_1}{\partial t} = \frac{1}{f_0^2 L} \int_{-L/2}^{L/2} \frac{\partial \phi_1}{\partial x} \frac{\partial^2 \phi_1}{\partial x \partial t} dx, \tag{21}$$

$$\frac{\partial K_3}{\partial t} = \frac{1}{f_0^2 L} \int_{-L/2}^{L/2} \frac{\partial \phi_3}{\partial x} \frac{\partial^2 \phi_3}{\partial x \partial t} dx, \tag{22}$$

and, from (19),

$$\frac{\partial K}{\partial t} = \frac{\partial K_1}{\partial t} + \frac{\partial K_3}{\partial t}. \tag{23}$$

We define,

$$\mu_1 \equiv \left(\frac{1}{K_1} \frac{\partial K_1}{\partial t} \right)_{t=0}, \tag{24}$$

$$\mu_3 \equiv \left(\frac{1}{K_3} \frac{\partial K_3}{\partial t} \right)_{t=0}, \tag{25}$$

$$\mu \equiv \left(\frac{1}{K} \frac{\partial K}{\partial t} \right)_{t=0}. \tag{26}$$

The initial values of K_1 , K_3 , and K may be determined by use of (14) and (15). Closed form expressions for the initial values of $\partial \phi_s / \partial t$ and $\partial \phi_D / \partial t$ (and, hence, for $\partial \phi_1 / \partial t$ and $\partial \phi_3 / \partial t$) may be found by use of (8, 9, 10, 11, 14 and 15). With these, the initial values of $\partial K_1 / \partial t$, $\partial K_3 / \partial t$, and $\partial K / \partial t$ may be found from equations (21, 22, 23). This procedure yields,

$$\mu_1 = \frac{[\beta \gamma^2 \sin \delta - \nu k (\eta k^2 + \gamma^2) \cos \delta]}{k M (k^2 + \gamma^2)}, \tag{27}$$

$$\mu_3 = \frac{\{\nu k [k^2 (\eta - 2) - \gamma^2] - \gamma^2 \beta M \sin \delta\}}{k (k^2 + \gamma^2)}, \tag{28}$$

$$\mu = \frac{\nu [k^2 (\eta - 2) - \gamma^2 - M (\eta k^2 + \gamma^2) \cos \delta]}{(M^2 + 1) (k^2 + \gamma^2)}. \tag{29}$$

To obtain these results, $\partial \phi_1 / \partial t$, $\partial \phi_3 / \partial t$, $\partial^{n+1} \phi_1 / \partial t \partial x^n$, and $\partial^{n+1} \phi_3 / \partial t \partial x^n$ ($n = 1, 2, 3 \dots$) were required to be cyclically continuous at $x = \pm L/2$. At the intersections of the convective and non-convective regions ($x = \pm L/4$), $\partial \phi_1 / \partial t$ and $\partial \phi_3 / \partial t$ were required to be continuous.

Since our interest is in systems which grow simultaneously at levels 1 and 3, we restrict ourselves to combinations of M and δ such that

$$\mu_1 = \mu_3 = \mu. \tag{30}$$

This, however, is not sufficient to insure that the percentage rate of change of kinetic energy will be the same at both levels over finite intervals of time since differences in phase speed between the two levels can quickly alter the initial phase lag. Therefore, we place an additional restriction on M and δ such that $C_1 = C_3$ where C_1 and C_3 are, respectively, the initial phase speeds at levels 1 and 3. Under these circumstances, equations (27), (28), (29) should not only give the initial percentage rates of change of kinetic energy but should also provide reliable information concerning changes over finite intervals of time.

For C_1 and C_3 , we take the initial translation of the geopotential lines which separate the convective and non-convective regions. Therefore,

$$C_1 = - \left[\frac{\partial \phi_1 / \partial \phi_1}{\partial t / \partial x} \right]_{t=0, x=\pm L/4}, \tag{31}$$

$$C_3 = - \left[\frac{\partial \phi_3 / \partial \phi_3}{\partial t / \partial x} \right]_{t=0, x=\pm L/4}. \tag{32}$$

These can be evaluated to yield

$$C_1 = - \frac{\beta [\gamma^2 + (2k^2 + \gamma^2) M \cos \delta]}{2k^2 (k^2 + \gamma^2) M \cos \delta}, \tag{33}$$

$$C_3 = - \frac{\beta [2k^2 + \gamma^2 (1 + M \cos \delta)]}{2k^2 (k^2 + \gamma^2)}. \tag{34}$$

For these phase speeds to be equal,

$$M \cos \delta = \pm 1. \tag{35}$$

By use of (29), the positive sign yields

$$\mu = \frac{2\nu}{M^2 + 1} \tag{36}$$

or cases which are in a state of decay at the initial instant. The negative sign leads to

$$\mu = \frac{2\nu k^2 (\eta - 1)}{(M^2 + 1) (k^2 + \gamma^2)} \tag{37}$$

which shows initial growth when $\eta > 1$.

For $\mu_1 = \mu_3$,

$$\beta \gamma^2 (1 + M^2) \sin \delta = \nu k M [k^2 (\eta - 2) - \gamma^2] + \nu k (\eta k^2 + \gamma^2) \cos \delta. \tag{38}$$

If we use $M \cos \delta = -1$ to eliminate δ from (38),

$$M^{*3} + \{1 - \nu^2 k^2 [k^2 (\eta - 2) - \gamma^2]^2 / \beta^2 \gamma^4\} M^{*2} + \{2\nu^2 k^2 [k^2 (\eta - 2) - \gamma^2] [\eta k^2 + \gamma^2] / \beta^2 \gamma^4 - 1\} M^* - \{1 + \nu^2 k^2 (\eta k^2 + \gamma^2)^2 / \beta^2 \gamma^4\} = 0 \tag{39}$$

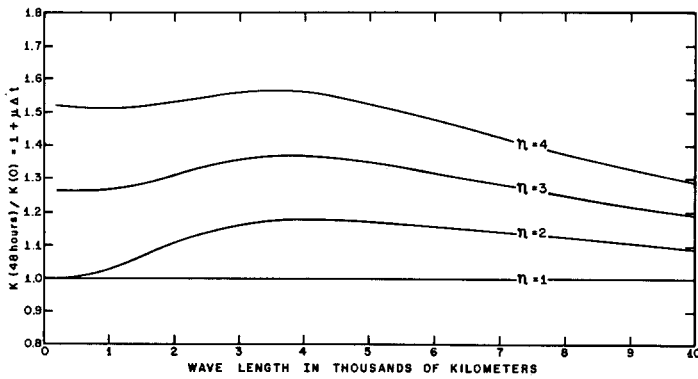


FIGURE 2.—Ratio of final to initial kinetic energy under the assumption that the initial kinetic energy tendency is preserved over a 48-hr. period. Ratios are equal to $1 + \mu\Delta t$, where $\Delta t = 48$ hr. and μ is calculated such that the initial percentage rates of change of kinetic energy and the initial phase speeds at levels 1 and 3 are equal.

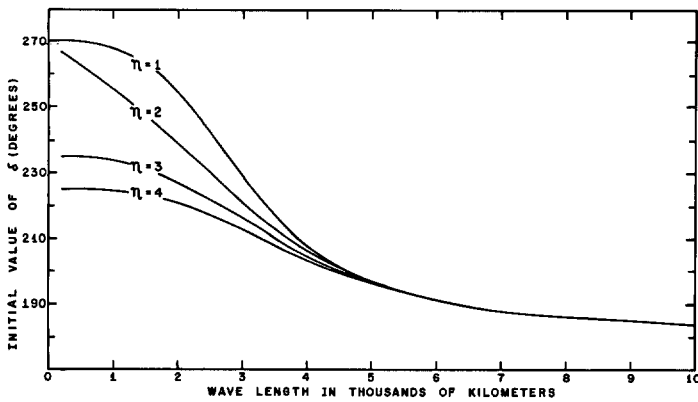


FIGURE 3.—Phase lags, δ , between geopotential patterns at levels 1 and 3 required to make initial percentage rates of change of kinetic energy and initial phase speeds equal at levels 1 and 3.

where

$$M^* = M^2, \quad M > 0. \quad (40)$$

Equation (39) will always have one or more real roots. In view of equations (35) and (40), the only physically significant roots are those which are real, positive, and greater than 1 in magnitude. For the values of the parameters employed here ($\beta = 2.14 \times 10^{-11} \text{ sec.}^{-1} \text{ m.}^{-1}$, $\sigma_2 = 3 \text{ m.t.s.}$, $D_E = 730 \text{ m.}$, $l^* = 0.7$, $\sin 2\psi = \frac{1}{2}$, $f_0 = 5 \times 10^{-5} \text{ sec.}^{-1}$, $200 \text{ km.} \leq L \leq 10,000 \text{ km.}$, $1 \leq \eta \leq 4$), it was always possible to find one or more physically significant roots. In the cases where more than one such root was found, the smallest value was adopted since, by (37), this gives the largest value of μ .

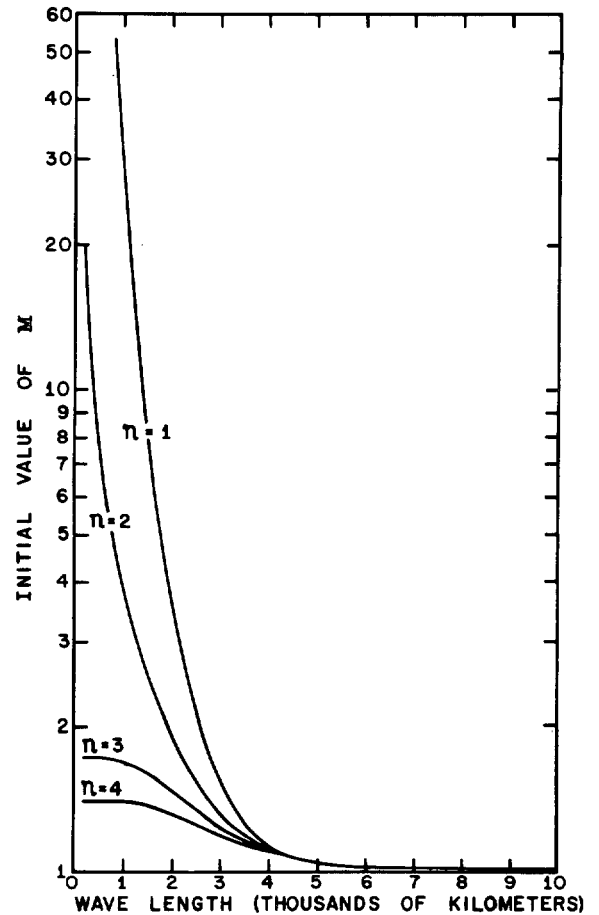


FIGURE 4.—Ratio of geopotential amplitudes, M , required to make initial percentage rates of change of kinetic energy and initial phase speeds equal at levels 1 and 3.

Once M has been determined from (39) and (40), $\cos \delta$ is calculated from $M \cos \delta = -1$ and $\sin \delta$ is obtained from (38). The angle δ is then completely determined.

4. RESULTS

Figure 2 shows values of $1 + \mu\Delta t$ ($\Delta t = 48$ hr.) which would be the ratio of final to initial kinetic energy if $\partial K / \partial t$ were preserved over a 48-hr. period. The values of μ are based on combinations of M and δ obtained as described in the previous section. The variations of μ with wavelength are extremely encouraging since the maxima are on the synoptic scale.

Figures 3 and 4 show, respectively, the corresponding values of δ and M . At a wavelength of 4000 km., which is

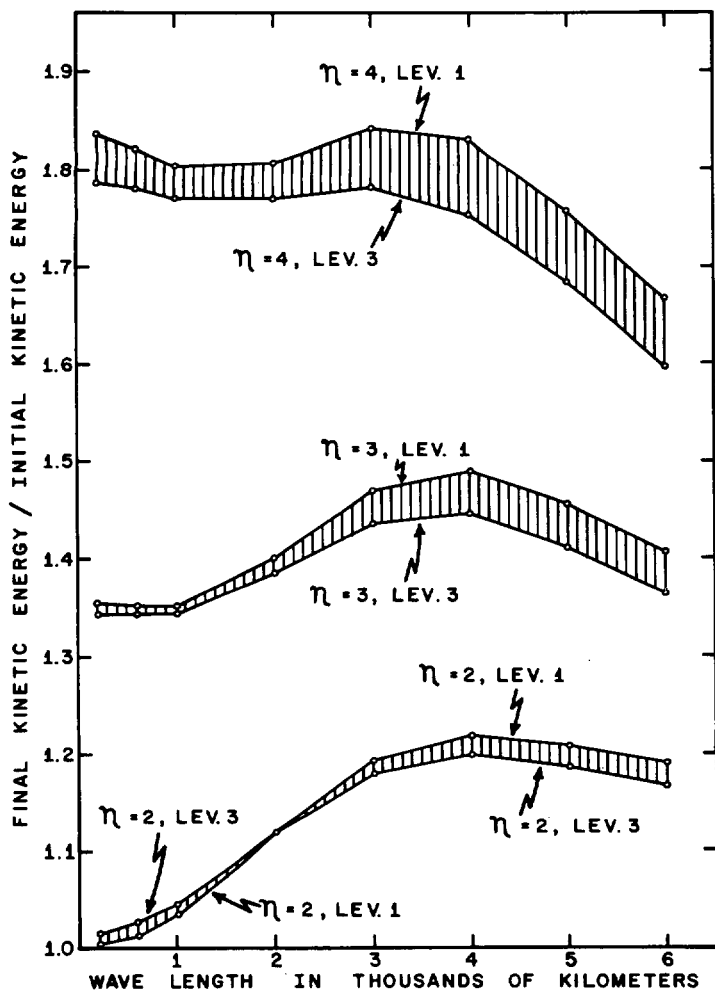


FIGURE 5.—Ratios of final kinetic energy to initial kinetic energy at levels 1 and 3 as obtained from numerical integration of the system of equations (7a), (7b), (7c), (8), (9), (10), (11). Initial values of M and δ are taken from figures 4 and 5.

close to that of maximum μ for $2 \leq \eta \leq 4$, the upper-level ridge is $\frac{1}{12}$ to $\frac{1}{18}$ of a wavelength to the west of the low-level trough. As pointed out earlier, observations seem to indicate that the upper-level anticyclogenesis occurs somewhat to the east of the low-level cyclogenesis. The theory, therefore, appears to be deficient in this respect.

The system of equations (8), (9), (10), (11), subject to the conditions (7a), (7b), (7c) were integrated numerically for $\eta=1, 2, 3, 4$; $L=200, 600, 1000, 2000, 3000, 4000, 5000$, and 6000 km. The initial conditions consisted of equations (14) and (15) with δ and M taken from figures 3 and 4, respectively. Numerical integration of this system is fairly straightforward and details will not be

given. We point out that 15 grid points were used in the zonal direction and that boundary conditions at $x = \pm L/2$ were cyclic continuity in $\partial\phi_0/\partial t$ and $\partial\phi_s/\partial t$. The integrations spanned 48 hr. The initial value of $(T_s - T_2)$ was taken as 5°C . $(T_s)_2$ was held constant with time.

Ratios of final to initial kinetic energy (per wavelength) are shown by figure 5. (The ratios for the $\eta=1$ cases fall in the range 0.998–1.001.) The following represents a summary of the more significant aspects of figure 5.

1. The time variations of kinetic energy are similar at both levels indicating that the analysis performed in the previous section produced initial conditions with the desired properties.

2. The criterion for growth appears to be $\eta > 1$ which is also in agreement with the analysis of the previous section.

3. The shapes of the curves are similar to those shown in figure 2. Maximum growth is found in the 3,000 to 5,000-km. band of wavelengths.

5. SUMMARY

Convective heating, if taken as dependent on convergence in the Ekman layer and employed within the framework of a two-level, quasi-geostrophic, linear model, can lead to simultaneous growth in the upper and lower troposphere given initial conditions of the type considered here. With these initial conditions, maximum growth occurs for wavelengths between 3000 and 5000 km. This result is in rough qualitative agreement with synoptic observations which seem to indicate that convective heating can lead not only to the formation of hurricanes but also to the initiation and intensification of low tropospheric cyclones and upper tropospheric anticyclones having dimensions on the order of thousands of kilometers.

Computer programs now being written at the National Hurricane Research Laboratory will allow us to carry out new calculations with the nonlinear equations and also to take into account the meridional variations of the perturbations.

REFERENCES

1. J. G. Charney and A. Eliassen, "A Numerical Method for Predicting the Perturbations of the Middle-Latitude Westerlies," *Tellus*, vol. 1, No. 2, May 1949, pp. 38–54.
2. J. G. Charney and A. Eliassen, "On the Growth of the Hurricane Depression," *Journal of the Atmospheric Sciences*, vol. 21, No. 1, Jan. 1964, pp. 68–74.
3. N. L. Frank, "Synoptic Case Study of Tropical Cyclogenesis Utilizing TIROS Data," *Monthly Weather Review*, vol. 91, No. 8, Aug. 1963, pp. 355–366.
4. H. L. Kuo, "On Formation and Intensification of Tropical Cyclones Through Latent Heat Release by Cumulus Convection," *Journal of the Atmospheric Sciences*, vol. 22, No. 1, Jan. 1965, pp. 40–63.

5. Y. Ogura, "Frictionally Controlled, Thermally Driven Circulations in a Circular Vortex with Application to Tropical Cyclones," *Journal of the Atmospheric Sciences*, vol. 21, No. 6, Nov. 1964, pp. 610-620.
6. K. Ooyama, "A Dynamical Model for the Study of Tropical Cyclone Development," *Geofisica Internacional*, vol. 4, No. 4, Apr.-Dec. 1964, pp. 187-198.
7. H. Riehl, "On Production of Kinetic Energy from Condensation Heating," *The Atmosphere and the Sea in Motion*, Rockefeller Institute Press with Oxford University Press, New York, 1959, pp. 381-399.

[Received January 16, 1967; revised April 19, 1967]

CORRECTION

No. 4, April 1967, p. 218: The last sentence on the page should read ". . . condensation levels were *lower* over the Bahama Islands . . ." instead of "higher".